



## ISTITUTO NAZIONALE DI RICERCA METROLOGICA Repository Istituzionale

Developments of the k0-NAA measurement model implemented in k0-INRIM software

*Original*

Developments of the k0-NAA measurement model implemented in k0-INRIM software / Di Luzio, Marco; Oddone, Massimo; D'Agostino, Giancarlo. - In: JOURNAL OF RADIOANALYTICAL AND NUCLEAR CHEMISTRY. - ISSN 0236-5731. - 331:10(2022), pp. 4251-4258. [10.1007/s10967-022-08476-x]

*Availability:*

This version is available at: 11696/75620 since: 2023-02-14T10:40:13Z

*Publisher:*

SPRINGER

*Published*

DOI:10.1007/s10967-022-08476-x

*Terms of use:*

This article is made available under terms and conditions as specified in the corresponding bibliographic description in the repository

*Publisher copyright*

(Article begins on next page)



# Developments of the $k_0$ -NAA measurement model implemented in k0-INRIM software

Marco Di Luzio<sup>1</sup> · Massimo Oddone<sup>2</sup> · Giancarlo D'Agostino<sup>1</sup>

Received: 27 April 2022 / Accepted: 2 August 2022 / Published online: 23 August 2022  
© The Author(s) 2022

## Abstract

The k0-INRIM software is a computer program that was recently developed to automatically evaluate combined uncertainty while performing mass fraction measurements adopting the  $k_0$ -standardization method of Neutron Activation Analysis. In this paper, significant developments of the adopted measurement model, following a complete revision of the detector characterization procedure, are reported. In particular, the efficiency ratio between monitor and analyte  $\gamma$ -emissions accounts for conversions between counting positions, extended sample geometry and self-absorption. In addition, true-coincidence summing, neutron flux gradient, moisture and blank corrections are included in the model. The developed measurement model is implemented in the latest k0-INRIM release; this greatly improves flexibility of the software in most of the common situations encountered in routine analysis without losing its inherent characteristic focused on uncertainty evaluation through propagation of covariances via sensitivity coefficients. A performance test was carried out by measuring the Au mass fraction of a cylindrical sample prepared from electronic waste material. Results obtained by counting the sample at different positions with respect to the detector end-cap are presented.

**Keywords**  $\gamma$ -Detection efficiency · Neutron activation analysis ·  $\gamma$ -Spectrometry ·  $k_0$ -Standardization · Uncertainty evaluation · Software automation

## Introduction

The  $k_0$ -standardization method allows to carry out multi-elemental Neutron Activation Analysis (NAA) by providing the opportunity to investigate a large number of analytes from a single co-irradiated monitor [1].

The inclination towards high automation and large sample throughput make the  $k_0$ -standardization a largely adopted

method for routinely analysis in many NAA laboratories worldwide.

The large amount of experimental data to be processed coupled to a rather complex measurement equation require the adoption of a software to manage the elaboration of results. Several homemade and a commercial software [2, 3] are available for users.

Among the homemade software, the k0-INRIM is an open-source computer program written in python language aimed to help NAA users to easily obtain GUM (Guide to the expression of Uncertainty in Measurement [4]) compliant uncertainty budgets while performing analysis via  $k_0$ -standardization method [5]. Differently from  $k_0$  software currently available, the k0-INRIM focuses on a frequently overlooked but crucial aspect of the measurement, the uncertainty evaluation.

On the other hand, the k0-INRIM 1.0 version is lacking some features that strongly limits versatility towards its routine use, the most prominent concerning the efficiency evaluation. In detail, the 1.0 version does not offer the opportunity to manage monitor and analyte samples acquired at different counting positions which is, on the contrary, extremely

---

✉ Marco Di Luzio  
m.diluzio@inrim.it

Massimo Oddone  
oddone@unipv.it

Giancarlo D'Agostino  
g.dagostino@inrim.it

<sup>1</sup> Istituto Nazionale Di Ricerca Metrologica (INRIM), Unit of Radiochemistry and Spectroscopy C/o Department of Chemistry, University of Pavia, via Taramelli 12, 27100 Pavia, Italy

<sup>2</sup> Department of Chemistry, University of Pavia, via Taramelli 12, 27100 Pavia, Italy

useful to find the best experimental setup when dealing with unknown samples. Moreover, true-coincidence corrections are not automatically computed, thus users need to evaluate them separately making even more difficult to deal with close sample-detector countings. Finally, samples are considered as point-sources regardless of their actual geometry, thus making unpractical working with extended samples.

In the framework of a participation to a software inter-comparison proposed by the International Atomic Energy Agency (IAEA) aiming at comparing the proficiency of various  $k_0$  software, the implemented equation model was developed following a revision of the detector characterization approach.

This work presents changes applied to the measurement model to solve the shortcomings previously recalled; additional corrections for self-absorption, neutron flux gradient, moisture and blank are discussed. As well, the outcome of a performance test carried out to investigate the suitability of the measurement model changes in real experimental conditions are reported.

It is worth noting that the upgraded measurement model still allows the propagation of uncertainties taking into account correlations; the output uncertainty budget lists all input parameters and points out their contribution to the combined uncertainty of the result. This is a useful feature for users to immediately spot main uncertainty sources.

## Updates of the measurement model

### Detection efficiency

The original  $k_0$  equation model, as proposed by its creators [1], requires the ratio of detection efficiencies,  $k_\epsilon$ , for the analyte and monitor  $\gamma$ -emissions at their geometrical counting positions; composition of analyte and monitor samples must be taken into account to evaluate self-absorption effects.

The measurement equation implemented in the k0-INRIM 1.0 version assumes monitor and analyte samples as point-sources counted at the same position. The efficiency ratio is modeled by the exponential of a 6-terms polynomial [5, 6]:

$$k_\epsilon = \exp\left(\sum_{i=1}^6 a_i (E_m^{2-i} - E_a^{2-i})\right), \quad (1)$$

where variables  $a_i$  are fitting parameters,  $E$  is  $\gamma$ -emission energy and subscripts m and a refer to monitor and analyte, respectively; values of  $a_i$  parameters, and corresponding

covariance matrix, are obtained by fitting the efficiency curve at reference position with the exponential of polynomial function.

The development of the measurement equation expands the approach described in [7] while maintaining the focus towards management of correlated parameters. In addition, extended geometry and self-absorption corrections are included in order to improve sample modelization at close counting positions.

The updated formula of the efficiency ratio, consists of five factors and is:

$$k_\epsilon = k_{\epsilon\Delta E} k_{\epsilon\Delta d} k_{\text{pos}} k_{\text{geo}} k_{\text{sa}}, \quad (2)$$

where  $k_{\epsilon\Delta E}$  converts the efficiency between monitor and analyte emissions spaced by an energy  $\Delta E$  at reference position,  $k_{\epsilon\Delta d}$  converts the efficiency between reference and nominal counting position vertically spaced by a distance  $\Delta d$  from the reference position,  $k_{\text{pos}}$  corrects for actual sample positioning with respect to the corresponding nominal counting position,  $k_{\text{geo}}$  corrects for extended sample geometry and  $k_{\text{sa}}$  corrects for  $\gamma$ -self-absorption, respectively. Apart from  $k_{\text{sa}}$  all factors in Eq. (2) are based on the characterization of the detector performed with a set of  $\gamma$ -sources covering a suitable energy range. The adopted  $\gamma$ -sources set might contain both certified and non-certified radionuclides and should provide as many free-coincidence emissions as possible. Positions where  $\gamma$ -sources are counted are named nominal counting positions: the farthest from detector end-cap is the reference position. Apart from reference, all nominal positions are characterized using only coincidence-free  $\gamma$ -emissions. Moreover, experimental positions where bottoms of the extended samples are counted during the analysis are named actual counting positions. Here and hereafter, counting positions are considered nominal unless differently specified.

Factors of Eq. (2) are hereafter discussed in detail.

The  $k_{\epsilon\Delta E}$  is the monitor to analyte efficiency ratio at reference position. The adopted formula is defined as in Eq. (1). The here-mentioned reference position determines the distance to which all other counting positions are referred to; it is chosen at the farthest counting distance in order to minimize possible true-coincidence effects.

The  $k_{\epsilon\Delta d}$  is the (i) analyte reference to counting efficiency ratio in case monitor is counted at reference or (ii) monitor counting to reference efficiency ratio in case analyte is counted at reference or (iii) unity in case analyte and monitor are both counted at reference. A further situation is possible in which (iv) neither the monitor nor the analyte are counted at reference position, and is obtained

from the combination of (i) and (ii); however, this is not yet implemented in the updated version of the k0-INRIM software upon which this work relies and it will be added in a future software update. The corresponding formulae are:

$$\begin{aligned}
 \text{(i)} \quad k_{\epsilon\Delta d} &= \exp\left(\sum_{i=1}^6 b_i E_a^{2-i}\right) \\
 \text{(ii)} \quad k_{\epsilon\Delta d} &= \left(\exp\left(\sum_{i=1}^6 b_i E_m^{2-i}\right)\right)^{-1} \\
 \text{(iii)} \quad k_{\epsilon\Delta d} &= 1 \\
 \text{(iv)} \quad k_{\epsilon\Delta d} &= \exp\left(\sum_{i=1}^6 b_i E_a^{2-i}\right) \left(\exp\left(\sum_{i=1}^6 b'_i E_m^{2-i}\right)\right)^{-1},
 \end{aligned} \tag{3}$$

where  $b_i$  are fitting parameters based on the detector characterization; they are evaluated as explained in [7]. In formula (iv) of Eq. (3), the apostrophe applied on  $b_i$  in the second factor is to point out that the two series of parameters ( $b_i$  and  $b'_i$ ) might have different values depending on the adopted counting positions. As expected, when sample and standard are instead acquired at the same counting position (other than reference)  $b_i = b'_i$ .

The  $k_{\text{pos}}$  is the monitor to analyte efficiency correction ratio due to actual sample positioning:

$$k_{\text{pos}} = \left(\frac{d_m - d'_{0m}}{d_m + \delta d_m - d'_{0m}}\right)^2 \left(\frac{d_a - d'_{0a}}{d_a + \delta d_a - d'_{0a}}\right)^{-2}, \tag{4}$$

where  $d$  is the distance between the nominal counting position and the detector end-cap,  $\delta d$  is the (small) distance difference between the actual counting position of sample and its nominal counting position and  $d'_0$  is the distance between the point-of-action within the detector crystal and the detector end-cap [6]. Since in the Cartesian coordinate system adopted for  $\gamma$ -counting the origin is at the end-cap,  $d$  values are positive and  $d'_0$  are negative. See Appendix 1 for details concerning the adopted efficiency correction formula.

The point-of-action within the detector is located following the procedure suggested in [6] by calculating the square root of count rate ratios,  $k_{C\Delta d}$ , between reference and nominal positions closer to the detector end-cap for coincidence free  $\gamma$ -emissions of the  $\gamma$ -sources set. The adopted equation model includes non-linearities occurring close to the detector:

$$\sqrt{k_{C\Delta d}} = c_2 d^2 + c_1 d + c_0, \tag{5}$$

where  $k_{C\Delta d} = \frac{C_{\text{ref}}}{C_d}$  and  $c_i$  are fitting parameters;  $C_{\text{ref}}$  and  $C_d$  are count rates at reference and counting positions, respectively.

Due to non-linearities, the  $d'_0$  trend over distance referred to a specific  $\gamma$ -energy,  $d'_{0E}$ , depends on counting position. The resulting formula, obtained by linearizing Eq. (5) at distance  $d$ , is:

$$d'_{0E} = \frac{c_2 d^2 - c_0}{2c_2 d + c_1}. \tag{6}$$

The dataset of  $d'_{0E}$  values obtained by Eq. (6) evaluated at the same counting position from all coincidence-free  $\gamma$ -emissions of the adopted source set is fitted with the following equation modeling the  $d'_0$  trend referred to a specific counting position,  $d'_{0d}$ , and depending on the energy of  $\gamma$ -emission:

$$d'_{0d} = -\exp\left(\sum_{i=1}^5 l_i E^{2-i}\right), \tag{7}$$

where  $l_i$  are fitting parameters.

Equation (7) is used in Eq. (4) to compute  $d'_0$  for monitor and analyte counting positions and  $\gamma$ -energies.

The  $k_{\text{geo}}$  is the monitor to analyte efficiency correction ratio due to extended cylindrical sample geometry:

$$k_{\text{geo}} = \left(1 + \frac{h_m}{d_m + \delta d_m - d'_{0m}}\right)^{-1} \left(1 + \frac{h_a}{d_a + \delta d_a - d'_{0a}}\right), \tag{8}$$

where  $h$  is the cylinder height. See Appendix 2 for details concerning the adopted efficiency correction formula.

The  $k_{\text{sa}}$  is the monitor to analyte self-absorption correction ratio according to the Debertain-Helmer formula [8]:

$$k_{\text{sa}} = \left(\frac{1 - e^{-\nu_m h_m \rho_m}}{\nu_m h_m \rho_m}\right) \left(\frac{1 - e^{-\nu_a h_a \rho_a}}{\nu_a h_a \rho_a}\right)^{-1}, \tag{9}$$

where  $\nu$  and  $\rho$  are the mass attenuation coefficient and density of the sample, respectively. Values of  $\nu$  are computed using information gathered from literature and sample composition:

$$\nu = \sum_{i=1} w_i \left(\frac{\mu}{\rho}\right)_i, \tag{10}$$

where  $w_i$  is the mass fraction of element  $i$  in the sample and  $(\mu/\rho)_i$  the mass attenuation coefficient of element  $i$  at the detected  $\gamma$ -energy;  $(\mu/\rho)_i$  values are conveniently recalled from a NIST database [9].

In summary, the detailed model of the implemented efficiency ratio,  $k_\epsilon$ , is:

$$\begin{aligned}
k_{\varepsilon} = & \exp\left(\sum_{i=1}^6 a_i(E_m^{2-i} - E_a^{2-i})\right) k_{\varepsilon\Delta d} \\
& \times \left(\frac{d_m - d'_{0m}}{d_m + \delta d_m - d'_{0m}}\right)^2 \left(\frac{d_a - d'_{0a}}{d_a + \delta d_a - d'_{0a}}\right)^{-2} \\
& \times \left(1 + \frac{h_m}{d_m + \delta d_m - d'_{0m}}\right)^{-1} \left(1 + \frac{h_a}{d_a + \delta d_a - d'_{0a}}\right) \\
& \times \left(\frac{1 - e^{-v_m h_m \rho_m}}{v_m h_m \rho_m}\right) \left(\frac{1 - e^{-v_a h_a \rho_a}}{v_a h_a \rho_a}\right)^{-1},
\end{aligned} \quad (11)$$

where  $k_{\varepsilon\Delta d}$  is defined in Eq. (3) depending on the counting scenario.

The uncertainty of  $k_{\varepsilon}$  is evaluated by propagating covariances of each input parameter indicated in Eq. (11) and, for what concerns  $k_{\varepsilon\Delta d}$ , indicated in Eq. (3), through their sensitivity coefficients.

### True-coincidence summing correction

In the k0-INRIM 1.0 version the correction for true-coincidence summing is included in the measurement model as an input parameter and its value is calculated manually by the user. Instead, the following true-coincidence correction formula based on De Corte's work [1] is implemented in the new version:

$$COI = \left(1 - \sum_i F_{\text{loss}}(i)\right) \left(1 + \sum_i F_{\text{sum}}(i)\right), \quad (12)$$

where  $COI$  is the true-coincidence correction factor,  $i$  indicates any cascade possibly involved in a coincidence with the detected  $\gamma$ ,  $F_{\text{loss}}$  and  $F_{\text{sum}}$  represent a pool of functions to evaluate loss and summing effects [1]. Literature data, full-energy peak efficiencies and  $P/T$  values, obtained from the detector characterization process, are used to calculate  $F_{\text{loss}}$  and  $F_{\text{sum}}$ .

The peak-to-total ( $P/T$ ) is a parameter defined as the ratio between net peak area and total counts of a background-corrected spectrum for a true-coincidence free  $\gamma$ -emitter. By acquisition of multiple mono-emitting  $\gamma$ -sources, a series of  $P/T$  data related to the same counting position are obtained upon which a fitting model is adjusted. According to the De Corte approach, the  $P/T$  versus  $\gamma$ -energy,  $E$ , fit is performed using a 2nd degree polynomial at low energies and a straight line at higher energies, on a log–log scale plot:

$$P/T = \begin{cases} 10^{p_1(\log_{10} E)^2 + p_2 \log_{10} E + p_3}, & 0 < E \leq E_j \\ 10^{s_1 \log_{10} E + s_2}, & E > E_j \end{cases}, \quad (13)$$

where  $E_j$  is the threshold energy,  $p$  and  $s$  are fitting parameters.

The  $s$  parameters are calculated first, afterwards,  $p$  fitting parameters are obtained by minimization of the sum of squared residuals.

As an original feature with respect to the widely adopted De Corte approach and in order to avoid discontinuities, values and first derivatives of the polynomial and straight line fitting equation are set equal at  $E_j$ ; with  $E_j$  adjustable by the user to minimize the residuals.

A fixed 20% relative uncertainty is preliminary assigned as a first tentative to both  $\sum_i F_{\text{loss}}(i)$  and  $\sum_i F_{\text{sum}}(i)$  and propagated to evaluate the combined uncertainty of the results. Users should be aware that the evaluation of the uncertainty of  $COI$  must be reconsidered in case it results to be among the most overriding ones in the uncertainty budget.

The true-coincidence correction here presented might not be suitable in case of very close source-detector distances and complicated decay schemes because of how the coincidence loss factor is expressed; in addition, the uncertainty evaluation is not rigorous due to the lack of uncertainty information in the adopted literature data. Developments to the  $COI$  correction will be considered for future implementations of the k0-INRIM measurement model.

### Flux gradient correction

The possibility to produce different activations for monitor and analytes due to their positions within the irradiation facility is not considered in equation model implemented in the k0-INRIM 1.0 version. Since in common nuclear reactors the largest variability is observed along the longitudinal axes of a channel [10, 11], a correction is introduced to take into account the expected count rate variations of monitor and analyte according to their vertical positions.

It is assumed that the thermal-to-epithermal flux ratio,  $f$ , and the departure from  $1/E$  epithermal trend,  $\alpha$ , are constant within the vertical segment of channel where analyte sample and its monitor sample are located, i.e. only the neutron flux intensity is allowed to change while the neutron energy distribution remains unchanged. Under these assumptions, the count rate correction,  $k_{\beta}$ , due to neutron flux vertical gradient is approximated with a linear trend:

$$k_{\beta} = 1 + \beta \Delta l_a, \quad (14)$$

where  $\beta$  is the vertical count rate gradient per unit distance and  $\Delta l_a$  is the distance between centers of mass of the analyte sample and the monitor sample within the irradiation facility.

The adopted formula for  $\beta$  is based on the activation and counting of two samples containing the same element with known mass fraction located close to the position where analyte and monitor samples are irradiated:

$$\beta = \frac{\Gamma_{sp1}/\Gamma_{sp2} - 1}{\Delta L_{12}}, \quad (15)$$

where  $\Gamma_{sp1}$  and  $\Gamma_{sp2}$  are (mass) specific emission rates of sample 1 and 2, respectively, and  $\Delta L_{12}$  is the distance between samples. The origin of the Cartesian coordinate system adopted for sample placement is at the bottom of the irradiation channel; accordingly,  $\Delta L_{12}$  is positive when sample 1 is located above sample 2.

The best accuracy is reached when the analyte sample is irradiated sandwiched between two monitor samples used for the evaluation of  $\beta$ .

The uncertainty of  $k_\beta$  is evaluated by propagating covariances of each input parameter indicated in Eq. (14) and, for what concerns  $\beta$ , indicated in Eq. (15), through their sensitivity coefficients.

### Other improvements

It is useful to mention two additional features included in the measurement model and accounting for corrections due to sample moisture and blank effects.

The dry mass (both for analyte and monitor samples),  $m_{dry}$ , is calculated according to:

$$m_{dry} = m(1 - \eta), \quad (16)$$

where  $m$  is the weighted mass and  $\eta = \frac{m_{H_2O}}{m}$  is the moisture to sample mass ratio.

The mass of analyte due to blank,  $m_{a\ blank}$ , is calculated according to:

$$m_{a\ blank} = m_{blank} w_{a\ blank}, \quad (17)$$

where  $m_{blank}$  is the mass of activated container (blank) and  $w_{a\ blank}$  is the mass fraction of analyte found in the blank.

The uncertainties of  $m_{dry}$  and  $m_{a\ blank}$  are evaluated by propagating covariances of each input parameter indicated in Eq. (16) and Eq. (17), respectively, through their sensitivity coefficients.

### k<sub>0</sub>-INRIM measurement model

The updated measurement model for direct activation-decay analytes is:

$$w_a = \frac{1}{m_{sm}(1 - \eta_{sm})} \left( \frac{\lambda \left( \frac{n_p/COI}{(1-e^{-\lambda t_i})} \right) e^{\mu(1-\eta/t_c)}}{(1-e^{-\lambda t_i})(1-e^{-\lambda t_c})} \Big|_a \right) e^{(\lambda_a - \lambda_m)t_{dm} + \lambda_a \Delta t_d} \\ \times \frac{1}{1 + \beta \Delta L_{12}} \frac{k_{0\ Au}(m) G_{th\ m} + \frac{G_{em}}{f} \left( \frac{Q_{0m} - 0.429}{E_{ra}^\alpha} + \frac{0.429}{0.55^\alpha(1+2\alpha)} \right)}{k_{0\ Au}(a) G_{th\ a} + \frac{G_{ea}}{f} \left( \frac{Q_{0a} - 0.429}{E_{ra}^\alpha} + \frac{0.429}{0.55^\alpha(1+2\alpha)} \right)} k_\epsilon \\ \times m_{std}(1 - \eta_{std}) w_m - m_{blank} w_{a\ blank}, \quad (18)$$

where  $k_\epsilon$  can be expanded as in Eq. (11). It is worth to note that the exponential  $e^{(\lambda_a - \lambda_m)t_{dm} + \lambda_a \Delta t_d}$  accounting for the correction ratio due to analyte and monitor decay times ( $t_{da}$  and  $t_{dm}$ ) is equivalent to the usual formula  $e^{\lambda_a t_{da} - \lambda_m t_{dm}}$ . However, it represents an easier way to deal with the partial correlation between  $t_{da}$  and  $t_{dm}$  by making explicit the common part,  $t_{dm}$ , and their difference,  $\Delta t_d = t_{dm} - t_{da}$ . Parameters that are not mentioned in this work are discussed in [5].

### Performance test

Among the plethora of updates to the measurement model, key features for what concerns its overall applicability in routine analysis are introduced by  $k_{\epsilon \Delta d}$ ,  $k_{pos}$ ,  $k_{geo}$  and  $k_{sa}$  parameters.

In order to check the performance, a preliminary test was performed by measuring the mass fraction of an analyte element by counting the sample at different positions.

A material composed of shredded electronic waste was used to prepare the analyte sample to quantify Au; a mass of about 170 mg (with 1.6% moisture content) was weighted, pressed in the shape of a cylindrical tablet with 1.2 mm height and 10 mm diameter, and placed in a polyethylene (PE) vial suitable for irradiation.

A 1000  $\mu\text{g mL}^{-1}$  Au solution was used to prepare two monitor samples: for each, 15 mg mass solution was pipetted on absorbent paper that was afterwards evaporated and sealed between two foils of adhesive tape. Monitor and analyte samples were weighted using an analytical balance; the analyte sample mass was measured after the tablet was produced whereas monitor masses were measured during the pipetting of the Au solution taking into account evaporation. The choice of Au as a monitor element to quantify Au in the sample makes negligible typical  $k_0$ -method influence factors such as  $k_0$ -related literature values, flux characterization, true-coincidence summing correction and allows to focus on the application of the formula adopted for  $k_\epsilon$ , Eq. (11), at least for the Au  $\gamma$ -line.

The analyte sample was sandwiched between the two monitor samples and tightly packed within a PE irradiation container by leaving 3 mm between their centers of mass; the bottom monitor sample is used as a standard, whereas

the upper monitor sample is used as an additional analyte sample and to calculate the flux gradient correction. The neutron irradiation took place in one of the channels situated in the carousel facility of TRIGA Mark II reactor of Pavia; the neutron exposure lasted 1 h at 250 kW power.

After suitable cooling time, multiple  $\gamma$ -spectra for monitor and analyte samples were acquired on an hyper-pure Ge (HPGe) detector (ORTEC, 50% relative efficiency, 1.90 keV resolution at 1332 keV energy, 66 mm crystal diameter) connected to an ORTEC DSPEC 502 and controlled by a personal computer running GammaVision software for spectra acquisition and HyperLab for peak elaboration.

The detection system was characterized according to the methodology described in this work and using a set of single radionuclides including certified ones ( $^{152}\text{Eu}$ ,  $^{133}\text{Ba}$ ,  $^{241}\text{Am}$ ,  $^{109}\text{Cd}$ ,  $^{57}\text{Co}$  and  $^{137}\text{Cs}$ ) and home-made ones for which the activity was measured at reference position ( $^{65}\text{Zn}$ ,  $^{51}\text{Cr}$  and  $^{198}\text{Au}$ ). A total of 10 nominal counting positions was settled, the reference being at 203.6 mm distance from detector end-cap while the others at steps of 20 mm down to 23.6 mm using calibrated spacers.

The bottom monitor sample was counted only at 203.6 mm (reference) whereas both the analyte sample and the upper monitor sample were counted at 203.6 mm, 103.6 mm, 63.6 mm and 23.6 mm. Actual counting positions were 0.4 mm above the nominal counting positions.

Au mass fraction values of the upper monitor and analyte samples quantified at 203.6 mm were regarded as reference values since they were obtained in best experimental conditions, i.e. negligible effects from positioning and sample geometry, and suitably low counting statistics was reached.

## Results

The outcome of the performance test is shown in Fig. 1 in terms of relative departures of the quantified Au mass fraction from the reference value,  $w_d w_{\text{ref}}^{-1}$ ; upper monitor and analyte samples data are plotted in the upper and lower graph, respectively.

The combined relative uncertainty reached is 0.7%, 0.8%, 0.8% and 1.3% for upper monitor and 0.7%, 0.7%, 1.7% and 4.1% for analyte sample at actual positions 204.0 mm, 104.0 mm, 64.0 mm and 24.0 mm, respectively. The main contributor to the combined uncertainty was counting statistics. In particular, a significant amount of Br in the shredded electronic waste material made it difficult the earlier  $\gamma$ -counting of the analyte sample at close counting position. A posteriori, since the  $^{198}\text{Au}/^{82}\text{Br}$  ratio improves with times, better results would have been possible with a better choice of measuring and counting times.

The observed 0.7%, 0.5%, 1.6% relative departures from reference of the upper monitor values and 0.7%, 0.85%,

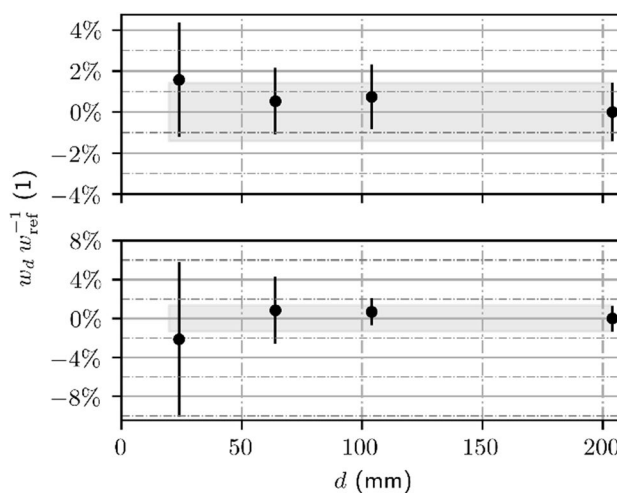


**Fig. 1** Relative departures of the quantified Au mass fraction from the reference value versus counting distance both for upper monitor sample (upper graph) and analyte sample (lower graph) with error bars indicating the expanded combined uncertainty ( $k=2$  coverage factor). The gray horizontal bands highlight the 95% confidence interval of reference value

**Table 1** List of relevant factors used to obtain  $k_\epsilon$ ,  $k_{\epsilon\Delta d}$  and  $k_{\text{pos}}$  are reported once since their values were the same for both analyte and monitor samples for the same counting positions; the  $k_{\text{geo}}$  column refers to the value estimated for analyte sample while for monitor sample the unity value was assigned at all counting positions. Digits in parenthesis represent the standard uncertainty of its corresponding value

$d(\text{mm})$	$k_{\epsilon\Delta d}(1)$	$k_{\text{pos}}(1)$	$k_{\text{geo}}(1)$
104.0	0.31967(94)	1.0026(40)	1.00866(79)
64.0	0.15506(43)	1.0052(49)	1.0125(11)
24.0	0.05033(23)	1.0118(83)	1.0174(19)

-2.1% of the analyte sample values quantified at 104.0 mm, 64.0 mm and 24.0 mm, respectively, are within the evaluated uncertainties and might suggest the suitability, up to the percent level, of the equation models for  $k_{\epsilon\Delta d}$ ,  $k_{\text{pos}}$  and  $k_{\text{geo}}$  parameters as defined in this study and the absence of major errors in the procedure.

The relevant  $k_{\epsilon\Delta d}$ ,  $k_{\text{pos}}$  and  $k_{\text{geo}}$  values calculated for all counting positions are reported in Table 1.

It is worth to note that, also in the most critical experimental condition, i.e. sample acquired at close detector distance, no dramatic departure, within the reported uncertainty, from the expected mass fraction value was pointed out. Despite the combined uncertainties obtained for the analyte and monitor samples are not satisfactory to validate the value of the applied corrections and the corresponding stated uncertainties they are still useful pieces

of information to confirm the suitability of modelization for these corrections at percent level.

## Conclusion

Developments of the measurement model improved significantly its suitability in real experimental conditions. The main change followed a completely revised detector characterization and concerned the capability to deal with different standard and sample counting positions, including corrections due to sample positioning, cylindrical extended geometry and self-absorption effects. True-coincidence summing, flux gradient, sample moisture and blank corrections were also introduced.

The upgraded measurement model has several additional input parameters deriving from the revised approach of efficiency characterization and additional features. Its development was carried out in such a way that its implementation in the new version of the k0-INRIM software retains the primary feature, i.e. the automatic production of GUM-compliant uncertainty budgets taking into account correlations among all input parameters.

## Appendix 1

Based on the quadratic attenuation formula, the adopted efficiency correction ratio of actual (defined by monitor and analyte placement during analysis) to nominal (defined by  $\gamma$ -sources placement during detector characterization) counting position is:

$$\frac{\varepsilon_{\text{act}}}{\varepsilon_{\text{nom}}} = \frac{1/D_{\text{act}}^2}{1/D_{\text{nom}}^2} = \left( \frac{d - d'_0}{d + \delta d - d'_0} \right)^2, \quad (19)$$

where  $\varepsilon$  is the efficiency for a point-like source and  $D$  is the distance between the point-like source and the point-of-action within the detector crystal.

Therefore, according to Eq. (19),  $k_{\text{pos}}$  results to be:

$$k_{\text{pos}} = \frac{\varepsilon_{\text{act m}}}{\varepsilon_{\text{nom m}}} \left( \frac{\varepsilon_{\text{act a}}}{\varepsilon_{\text{nom a}}} \right)^{-1}. \quad (20)$$

## Appendix 2

Based on the quadratic attenuation formula, the adopted efficiency correction for extended cylindrical sample geometry is the extended volume to point-like efficiency ratio:

$$\frac{\varepsilon_{\text{vol}}}{\varepsilon_{\text{point}}} = \frac{h^{-1} \int_D^{D+h} x^{-2} dx}{1/D^2} = \left( 1 + \frac{h}{D} \right)^{-1}, \quad (21)$$

where,  $\varepsilon_{\text{vol}}$  is the efficiency for a cylindrical sample with bottom located at distance  $D$  from point-of-action of detector and  $\varepsilon_{\text{point}}$  is the efficiency for the point-like sample at  $D$ .

It is worth to note that the efficiency correction models the situation in which the diameter and height of the cylinder are negligible with respect to detector diameter and counting distance, respectively.

Therefore, according to Eq. (21),  $k_{\text{geo}}$  results to be:

$$k_{\text{geo}} = \frac{\varepsilon_{\text{vol m}}}{\varepsilon_{\text{point m}}} \left( \frac{\varepsilon_{\text{vol a}}}{\varepsilon_{\text{point a}}} \right)^{-1}. \quad (22)$$

**Funding** Open access funding provided by Istituto Nazionale di Ricerca Metrologica within the CRUI-CARE Agreement.

## Declarations

**Conflict of interest** The authors have no competing interests to declare that are relevant to the content of this article.

**Open Access** This article is licensed under a Creative Commons Attribution 4.0 International License, which permits use, sharing, adaptation, distribution and reproduction in any medium or format, as long as you give appropriate credit to the original author(s) and the source, provide a link to the Creative Commons licence, and indicate if changes were made. The images or other third party material in this article are included in the article's Creative Commons licence, unless indicated otherwise in a credit line to the material. If material is not included in the article's Creative Commons licence and your intended use is not permitted by statutory regulation or exceeds the permitted use, you will need to obtain permission directly from the copyright holder. To view a copy of this licence, visit <http://creativecommons.org/licenses/by/4.0/>.

## References

1. De Corte F (1987) The  $k_0$ -standardization method. Rijksuniversiteit, Gent
2. Roszbach M, Blaauw M, Bacchi MA, Lin X (2007) The  $k_0$ -IAEA program. J Radioanal Nucl Chem 274:657–662
3. De Corte F, van Sluijs R, Simonits A, Kucera J, Smodis B, Byrne AR (2001) Installation and calibration of Kayzero-assisted NAA in three central European countries via a Copernicus project. Appl Radiat Isot 55:347–354
4. JCGM (2008) Evaluation of measurement data – Guide to the expression of uncertainty in measurement. BIPM, Sevres
5. D'Agostino G, Di Luzio M, Oddone M (2020) The k0-INRIM software: a tool to compile uncertainty budgets in Neutron Activation Analysis based on  $k_0$ -standardisation. Meas Sci Technol 31:1–4
6. Gilmore G (2008) Practical gamma-ray spectrometry. Wiley, Warrington



7. Di Luzio M, D'Agostino G, Oddone M (2020) A method to deal with correlations affecting  $\gamma$ -counting efficiencies in analytical chemistry measurements performed by  $k_0$ -NAA. *Meas Sci Technol*. <https://doi.org/10.1088/1361-6501/ab7ca8>
8. Debertin K, Helmer RG (1988) *Gamma- and X-ray spectrometry with semiconductor detectors*. North Holland, Amsterdam
9. Hubbell JH, Seltzer SM (1995) Tables of X-ray mass attenuation coefficients and mass energy-absorption coefficients from 1 keV to 20 MeV for element Z=1 to 92 and 48 additional substances of domestic interest. NIST standard reference database 126. <https://doi.org/10.18434/T4D01F>
10. Di Luzio M, D'Agostino G, Oddone M, Salvini A (2019) Vertical variations of flux parameters in irradiation channels at the TRIGA Mark II reactor of Pavia. *Prog Nucl Energy* 113:247–254
11. Bode P, Blaauw M, Obrusnik I (1992) Variation of neutron flux and related parameters in an irradiation channel container, in use with  $k_0$ -based Neutron Activation Analysis. *J Radioanal Nucl Chem* 157:301–312

**Publisher's Note** Springer Nature remains neutral with regard to jurisdictional claims in published maps and institutional affiliations.